hep-lat/9611015 15 Nov 1996

OUTP 96-64P
CERN-TH/96-312
DESY 96-222
FSU-SCRI-96-116

Non-perturbative determination of the axial current normalization constant in O(a) improved lattice QCD

Martin Lüscher[a], Stefan Sint[b], Rainer Sommer[c,d] and Hartmut Wittig[e]

[a] Deutsches Elektronen-Synchrotron DESY,
Notkestrasse 85, D-22603 Hamburg, Germany

[b] SCRI, The Florida State University, Tallahassee, FL 32306-4052, USA

[c] CERN, Theory Division, CH-1211 Genève 23, Switzerland

[d] DESY-IfH Zeuthen, Platanenallee 6, D-15738 Zeuthen, Germany

[e] Theoretical Physics, University of Oxford,
1 Keble Road, Oxford OX1 3NP, England

Abstract

A finite-size technique is employed to compute the normalization constant $Z_{\rm A}$ of the isovector axial current in lattice QCD. The calculation is carried out in the quenched approximation for values of the bare gauge coupling g_0 ranging from 0 to 1. In the lattice action and the lattice expression for the axial current we include the counterterms required for O(a) improvement, with non-perturbatively determined coefficients. With little additional work the normalization constant $Z_{\rm V}$ of the improved isospin current is also obtained.

November 1996

1. Introduction

In lattice QCD with Wilson quarks the conservation of the isovector axial current is violated by lattice effects. As a consequence a finite renormalization of the current is required to ensure that the chiral Ward identities assume their canonical form [1,2]. It is evidently important to compute the associated normalization constant $Z_{\rm A}$, since it contributes directly to physical matrix elements such as the pion decay constant F_π.

In perturbation theory $Z_{\rm A}$ has been worked out to one-loop order for various lattice actions and lattice definitions of the axial current [3–7]. The results may be used to calculate $Z_{\rm A}$ at the couplings of interest, but since these are not small in general it is difficult to say how reliable the numbers are that one obtains. A non-perturbative determination of the normalization constant is clearly preferable. Two different strategies to perform such a calculation have been pursued. In the first case $Z_{\rm A}$ is fixed by requiring certain chiral Ward identities between correlation functions of the axial and vector currents to be satisfied on the lattice [2,8–10]. The correlation functions are then evaluated through numerical simulation. The other proposition is to compute matrix elements of the axial current between quark states and to determine the normalization of the current by matching the numerical results with renormalized perturbation theory at large momentum transfers [11].

Our principal aim in the present paper is to calculate $Z_{\rm A}$ in the on-shell $\mathrm{O}(a)$ improved lattice theory. The significance of improvement in this context has previously been stressed in refs. [12–14]. Here we employ the improved action and the improved axial current with non-perturbatively determined $\mathrm{O}(a)$ counterterms [15–18]. All calculations are carried out in the quenched approximation. We use the Ward identity method and combine it with a finite-size technique based on the Schrödinger functional. This allows us to set the quark mass to zero (or to values very close to zero) and to determine $Z_{\rm A}$ at all bare couplings g_0 between 0 and 1. Contact with perturbation theory can thus be made.

For the definition of the Schrödinger functional and the $\mathrm{O}(a)$ improved theory the reader is referred to ref. [16]. The notations introduced there are taken over completely without further notice. In sect. 2 we briefly recall the euclidean Ward identities associated with the chiral symmetry of QCD in the continuum limit. We then define the isospin vector and axial vector currents in the on-shell $\mathrm{O}(a)$ improved lattice theory and derive the normalization conditions that will be used to compute the associated normalization constants

(sect. 3). As discussed in sect. 4 a careful interpretation of the rôle played by the current normalization conditions is required on the lattice, because the chiral Ward identities are only valid up to cutoff effects of order a^2. The calculation of the isospin vector and axial vector current normalization constants through numerical simulations is described in sects. 5 and 6. The paper ends with a few concluding remarks and a technical appendix, where an essentially rigorous proof of the crucial Ward identity is given.

2. Euclidean current algebra

We first consider the theory in the continuum limit and proceed formally, i.e. without paying attention to the proper definition of the correlation functions that occur. The boundary conditions on the quark and gluon fields do not matter in this section. We assume that there is an isospin doublet of quarks with mass m and study the associated chiral symmetry of the theory.

The isospin vector and axial vector variations of the quark and anti-quark field are defined by

$$\delta_{\mathrm{V}}^a \psi(x) = \tfrac{1}{2}\tau^a \psi(x), \qquad \delta_{\mathrm{V}}^a \overline{\psi}(x) = -\overline{\psi}(x)\tfrac{1}{2}\tau^a, \tag{2.1}$$

$$\delta_{\mathrm{A}}^a \psi(x) = \tfrac{1}{2}\tau^a \gamma_5 \psi(x), \qquad \delta_{\mathrm{A}}^a \overline{\psi}(x) = \overline{\psi}(x)\gamma_5 \tfrac{1}{2}\tau^a, \tag{2.2}$$

where τ^a denotes a Pauli matrix acting on the flavour indices of the quark field. The definition extends to arbitrary expressions $\mathcal{O}$ by treating δ_{V}^a and δ_{A}^a as first order differential operators. In particular, for the variations of the isospin vector and axial vector currents,

$$V_\mu^a(x) = \overline{\psi}(x)\gamma_\mu \tfrac{1}{2}\tau^a \psi(x), \qquad A_\mu^a(x) = \overline{\psi}(x)\gamma_\mu\gamma_5 \tfrac{1}{2}\tau^a \psi(x), \tag{2.3}$$

one obtains

$$\delta_{\mathrm{V}}^a V_\mu^b(x) = -i\epsilon^{abc} V_\mu^c(x), \qquad \delta_{\mathrm{A}}^a V_\mu^b(x) = -i\epsilon^{abc} A_\mu^c(x), \tag{2.4}$$

$$\delta_{\mathrm{V}}^a A_\mu^b(x) = -i\epsilon^{abc} A_\mu^c(x), \qquad \delta_{\mathrm{A}}^a A_\mu^b(x) = -i\epsilon^{abc} V_\mu^c(x). \tag{2.5}$$

The currents thus form a closed algebra under these variations.

The Ward identities associated with the chiral symmetry of the action are derived by performing local infinitesimal symmetry transformations of the quark and anti-quark fields in the euclidean functional integral. We choose to write the identities in an integrated form which is quite intuitive and will prove useful later on when we discuss the lattice theory.

Let R be a space-time region with smooth boundary ∂R. Suppose $\mathcal{O}_{\rm int}$ and $\mathcal{O}_{\rm ext}$ are polynomials in the basic fields localized in the interior and exterior of R respectively. The general vector current Ward identity then reads

$$\int_{\partial R} \mathrm{d}\sigma_\mu(x)\ \left\langle V^a_\mu(x)\mathcal{O}_{\rm int}\mathcal{O}_{\rm ext}\right\rangle = -\left\langle(\delta^a_{\rm V}\mathcal{O}_{\rm int})\,\mathcal{O}_{\rm ext}\right\rangle, \tag{2.6}$$

while for the axial current one obtains

$$\int_{\partial R} \mathrm{d}\sigma_\mu(x)\ \left\langle A^a_\mu(x)\mathcal{O}_{\rm int}\mathcal{O}_{\rm ext}\right\rangle = -\left\langle(\delta^a_{\rm A}\mathcal{O}_{\rm int})\,\mathcal{O}_{\rm ext}\right\rangle + 2m\int_R \mathrm{d}^4x\ \left\langle P^a(x)\mathcal{O}_{\rm int}\mathcal{O}_{\rm ext}\right\rangle. \tag{2.7}$$

The integration measure $\mathrm{d}\sigma_\mu(x)$ points along the outward normal to the surface ∂R and the pseudo-scalar density $P^a(x)$ is defined by

$$P^a(x) = \overline{\psi}(x)\gamma_5\tfrac{1}{2}\tau^a\psi(x). \tag{2.8}$$

The left-hand sides of eqs. (2.6) and (2.7) may be interpreted as matrix elements of the charge operators associated with the currents. This is made particularly clear if we choose R to be the space-time volume between two equal-time hyper-planes.

For illustration we set the quark mass to zero and choose $\mathcal{O}_{\rm int}$ to be one of the currents at some point y in the interior of R. An example of the resulting identities then is

$$\int_{\partial R} \mathrm{d}\sigma_\mu(x)\ \left\langle A^a_\mu(x)A^b_\nu(y)\mathcal{O}_{\rm ext}\right\rangle = i\epsilon^{abc}\left\langle V^c_\nu(y)\mathcal{O}_{\rm ext}\right\rangle, \tag{2.9}$$

and three more such relations, corresponding to eqs. (2.4) and (2.5), may be obtained. In this way the current algebra, which one usually sets up in Minkowski space in an operator language, is recovered in the euclidean domain.

3. Currents in lattice QCD

As already mentioned in sect. 1 we choose Wilson's formulation of lattice QCD and include all O(a) correction terms that are required for on-shell improvement. The lattice action etc. is exactly as in ref. [16]. We assume that the coefficients multiplying the O(a) counterterms have been adjusted so that the residual cutoff effects are of order a^2.

3.1 Improved currents

On the lattice the bare currents, V_μ^a and A_μ^a, are defined through the local expressions (2.3). The unrenormalized on-shell O(a) improved currents are then given by [15,16]

$$(V_{\rm I})_\mu^a = V_\mu^a + c_{\rm V} a \tfrac{1}{2}(\partial_\nu^* + \partial_\nu) T_{\mu\nu}^a, \tag{3.1}$$

$$(A_{\rm I})_\mu^a = A_\mu^a + c_{\rm A} a \tfrac{1}{2}(\partial_\mu^* + \partial_\mu) P^a. \tag{3.2}$$

For the anti-symmetric tensor field $T_{\mu\nu}^a$ we can take

$$T_{\mu\nu}^a(x) = i\overline{\psi}(x)\sigma_{\mu\nu}\tfrac{1}{2}\tau^a\psi(x), \tag{3.3}$$

while the axial density P^a is again defined through eq. (2.8).

The renormalization of lattice QCD is particularly transparent if a mass-independent renormalization scheme is employed. As discussed in sect. 3 of ref. [16] the renormalized improved currents in such schemes are given by

$$(V_{\rm R})_\mu^a = Z_{\rm V}(1 + b_{\rm V} a m_{\rm q})(V_{\rm I})_\mu^a, \tag{3.4}$$

$$(A_{\rm R})_\mu^a = Z_{\rm A}(1 + b_{\rm A} a m_{\rm q})(A_{\rm I})_\mu^a. \tag{3.5}$$

The renormalization constants $Z_{\rm V}$ and $Z_{\rm A}$ are functions of the modified bare coupling

$$\tilde{g}_0^2 = g_0^2(1 + b_{\rm g} a m_{\rm q}), \tag{3.6}$$

while $b_{\rm V}$, $b_{\rm A}$ and $b_{\rm g}$ depend on g_0 and should be adjusted so as to cancel any remaining cutoff effects of order $am_{\rm q}$. We shall not need to know these coefficients here, because the quark mass will be set to zero for the calculation of $Z_{\rm V}$ and $Z_{\rm A}$.

3.2 Normalization condition for the vector current

Although the isospin symmetry of the continuum theory is preserved on the lattice, the improved vector current introduced above is only conserved up to cutoff effects of order a^2. Its normalization is hence not naturally given and we must impose a normalization condition to fix $Z_{\rm V}$. Our aim in the following is to derive such a condition by studying the action of the renormalized isospin charge on states with definite isospin quantum numbers.

The matrix elements that we shall consider are constructed in the framework of the Schrödinger functional (see ref. [16] for details). We use the boundary field products

$$\mathcal{O}^a = a^6 \sum_{\mathbf{u},\mathbf{v}} \bar{\zeta}(\mathbf{u})\gamma_5 \tfrac{1}{2}\tau^a \zeta(\mathbf{v}), \tag{3.7}$$

$$\mathcal{O}'^a = a^6 \sum_{\mathbf{u},\mathbf{v}} \bar{\zeta}'(\mathbf{u})\gamma_5 \tfrac{1}{2}\tau^a \zeta'(\mathbf{v}), \tag{3.8}$$

to create initial and final states that transform according to the vector representation of the exact isospin symmetry. The correlation function

$$f_{\rm V}^{\rm R}(x_0) = \frac{a^3}{6L^6} \sum_{\mathbf{x}} i\epsilon^{abc} \langle \mathcal{O}'^a (V_{\rm R})_0^b(x) \mathcal{O}^c \rangle \tag{3.9}$$

can then be interpreted as a matrix element of the renormalized isospin charge between such states. The charge generates an infinitesimal isospin rotation (if properly normalized) and after some algebra one finds that the correlation function must be equal to

$$f_1 = -\frac{1}{3L^6} \langle \mathcal{O}'^a \mathcal{O}^a \rangle. \tag{3.10}$$

Strictly speaking this argumentation is only correct in the continuum theory. We may however conclude that

$$f_{\rm V}^{\rm R}(x_0) = f_1 + {\rm O}(a^2), \tag{3.11}$$

since the lattice correlation functions approach the continuum limit with a rate proportional to a^2. Note that we do not need to include the renormalization factors for the boundary quark fields here because they cancel in eq. (3.11).

The $\mathrm{O}(a)$ counterterm appearing in the definition (3.1) of the improved vector current does not contribute to the correlation function $f_{\mathrm{V}}^{\mathrm{R}}(x_0)$. So if we introduce the analogous correlation function for the bare current,

$$f_{\mathrm{V}}(x_0) = \frac{a^3}{6L^6} \sum_{\mathbf{x}} i\epsilon^{abc} \langle \mathcal{O}'^a V_0^b(x) \mathcal{O}^c \rangle, \tag{3.12}$$

it follows from eq. (3.11) that

$$Z_{\mathrm{V}}(1 + b_{\mathrm{V}} a m_{\mathrm{q}}) f_{\mathrm{V}}(x_0) = f_1 + \mathrm{O}(a^2). \tag{3.13}$$

By evaluating the correlation functions f_1 and $f_{\mathrm{V}}(x_0)$ through numerical simulation one is thus able to compute the normalization factor $Z_{\mathrm{V}}(1 + b_{\mathrm{V}} a m_{\mathrm{q}})$. In particular, to calculate Z_{V} it suffices to consider the theory at vanishing quark mass.

3.3 Normalization condition for the axial current

To derive a normalization condition for Z_{A}, we set the quark mass to zero from the beginning. Our starting point is the Ward identity (2.9) which we now write in the form

$$\int_{\partial R} \mathrm{d}\sigma_\mu(x)\, \epsilon^{abc} \left\langle A_\mu^a(x) A_\nu^b(y) \mathcal{O}_{\mathrm{ext}} \right\rangle = 2i \left\langle V_\nu^c(y) \mathcal{O}_{\mathrm{ext}} \right\rangle. \tag{3.14}$$

One may be hesitant to make use of this relation, since it has been deduced in a formal manner. A general argument, presented in appendix A, however shows that such worries are not justified. There is little doubt that eq. (3.14) is a true property of the theory in the continuum limit and so may be used to fix the normalization of the axial current on the lattice.

We now pass to the lattice theory and assume Schrödinger functional boundary conditions as before. A convenient choice of the region R is the space-time volume between the hyper-planes at $x_0 = y_0 \pm t$. From eq. (3.14) and $\mathrm{O}(a)$ improvement we then expect that

$$a^3 \sum_{\mathbf{x}} \epsilon^{abc} \left\langle [(A_{\mathrm{R}})_0^a(y_0 + t, \mathbf{x}) - (A_{\mathrm{R}})_0^a(y_0 - t, \mathbf{x})] (A_{\mathrm{R}})_0^b(y) \mathcal{O}_{\mathrm{ext}} \right\rangle$$

$$= 2i \left\langle (V_{\mathrm{R}})_0^c(y) \mathcal{O}_{\mathrm{ext}} \right\rangle + \mathrm{O}(a^2). \tag{3.15}$$

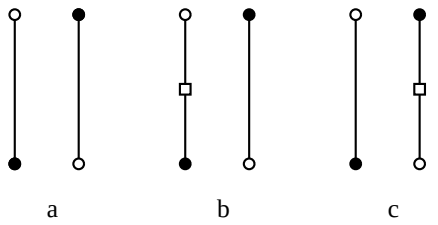

Fig. 1. Quark diagrams contributing to f_1 (diagram a) and $f_{\rm V}(x_0)$ (diagrams b and c). Filled (open) circles represent the creation (annihilation) of a quark at the boundaries of the lattice. The squares indicate the vector current insertions.

It has been important here that the fields in the correlation functions are localized at non-zero distances from each other. Since the theory is only on-shell improved, one would otherwise not be able to say that the error term is of order a^2 (cf. sect. 2 of ref. [16]).

After summing over the spatial components of y, and using the fact that the axial charge is conserved at zero quark mass (up to corrections of order a^2), eq. (3.15) becomes

$$a^6 \sum_{\mathbf{x},\mathbf{y}} \epsilon^{abc} \left\langle (A_{\rm R})^a_0(x) (A_{\rm R})^b_0(y) \mathcal{O}_{\rm ext} \right\rangle =$$

$$a^3 \sum_{\mathbf{y}} i \left\langle (V_{\rm R})^c_0(y) \mathcal{O}_{\rm ext} \right\rangle + {\rm O}(a^2), \tag{3.16}$$

where $x_0 = y_0 + t$. We now choose the field product $\mathcal{O}_{\rm ext}$ so that the function $f_{\rm V}^{\rm R}(y_0)$ introduced previously appears on the right-hand side of eq. (3.16). The normalization condition for the vector current then allows us to replace the correlation function by f_1. Explicitly, we define

$$f_{\rm AA}^{\rm I}(x_0, y_0) = -\frac{a^6}{6L^6} \sum_{\mathbf{x},\mathbf{y}} \epsilon^{abc} \epsilon^{cde} \left\langle \mathcal{O}'^d (A_{\rm I})^a_0(x) (A_{\rm I})^b_0(y) \mathcal{O}^e \right\rangle \tag{3.17}$$

and conclude from the above that

$$Z_{\rm A}^2 f_{\rm AA}^{\rm I}(x_0, y_0) = f_1 + {\rm O}(a^2) \tag{3.18}$$

for all times $x_0 > y_0$ between 0 and T. The normalization constant $Z_{\rm A}$ can thus be determined by computing the correlation functions f_1 and $f_{\rm AA}^{\rm I}(x_0, y_0)$ at zero quark mass.

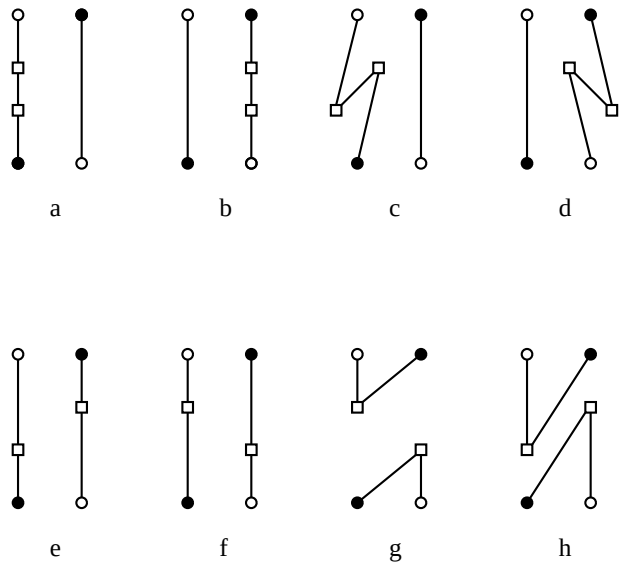

Fig. 2. Quark diagrams contributing to $f_{\rm AA}^{\rm I}(x_0,y_0)$. The squares indicate the axial current insertions at time x_0 (upper square) and y_0 (lower square).

3.4 Disconnected diagrams and the strange quark

As usual the integration over the quark and anti-quark fields in the functional integral is carried out analytically. One is then left with an integration over all gauge fields, the correlation functions f_1 etc. being given by a set of quark diagrams that correspond to the possible Wick contractions of the quark and anti-quark fields. For Schrödinger functional boundary conditions the required two-point contractions have been worked out in detail in sect. 2 of ref. [17].

In the case of f_1 and $f_{\rm V}(x_0)$ the assignment of the isospin quantum numbers is such that no disconnected quark diagrams appear (see fig. 1). The correlation function $f_{\rm AA}^{\rm I}(x_0,y_0)$ involves two current insertions and many more Wick contractions exist. Among the diagrams listed in fig. 2 there are also two disconnected ones (diagrams g and h). The isospin factors associated with the diagrams e and f vanish so that they can be dropped immediately.

We would now like to show that the disconnected diagrams do not contribute either. To this end we introduce a third quark, referred to as the strange quark, and replace the field products $\mathcal{O}'^a$ and $\mathcal{O}^a$ in the definitions of f_1 and $f_{\rm AA}^{\rm I}(x_0,y_0)$ by products of a strange and an isospin doublet quark boundary field. With appropriately contracted indices, the argumentation

leading to eq. (3.18) then goes through unchanged. Note that the currents are the same as before and the calculated value of $Z_{\rm A}$ must hence come out to be the same up to terms of order a^2. Since the strange quark does not couple to the axial current, the number of possible Wick contractions is strongly reduced and only the diagrams a and c survive, the line without current insertions representing the strange quark propagator. If we interchange quarks and anti-quarks one obtains the diagrams b and d instead. The isospin factors associated with the diagrams can be worked out straightforwardly and a comparison of the situation with and without strange quark then shows that the total contribution of the disconnected diagrams must vanish up to terms of order a^2.

In the course of the numerical computations described later in this paper, we have been able to verify that the disconnected diagrams indeed add up to zero within small statistical errors. We have thus decided to drop them and to extract $Z_{\rm A}$ from the connected part of $f_{\rm AA}^1(x_0,y_0)$.

4. Lattice effects and current normalization

The relations (3.13) and (3.18) determine the current normalization constants $Z_{\rm V}$ and $Z_{\rm A}$ only up to cutoff effects of order a^2. Depending on the choice of the lattice size, the boundary values of the gauge field and the other kinematical parameters that one has, slightly different results for $Z_{\rm V}$ and $Z_{\rm A}$ are hence obtained. One may try to assign a systematic error to the normalization constants by studying these variations in detail, but since there is no general rule as to which choices of the kinematical parameters are considered to be reasonable, such error estimates are bound to be rather subjective.

In our opinion the better way to deal with the problem is to *define* the normalization constants through a particular normalization condition. The physical matrix elements of the renormalized currents that one is interested in must then be calculated for a range of lattice spacings so as to be able to extrapolate the data to the continuum limit. The results obtained in this way are guaranteed to be independent of the chosen normalization condition, because any differences in the normalization constants of order a^2 extrapolate to zero together with the cutoff effects associated with the matrix elements themselves.

In the following we shall adopt this point of view and the precise choices that we shall make are then not too important. Some care must be paid to ensure that the cutoff effects in matrix elements of the renormalized currents between low-energy states are not artificially enhanced through an inappropriate choice of the kinematical parameters in eqs. (3.13) and (3.18). In particular, the external length scales (the time difference $x_0 - y_0$ and the lattice size, for example) should be sufficiently large compared to the lattice spacing, at all bare couplings considered. Perturbation theory can serve as a guide here and further confidence can be gained by studying the magnitude of the residual cutoff effects in various matrix elements of the renormalized currents through numerical simulations.

5. Numerical evaluation of f_1, $f_{\rm V}$ and $f_{\rm AA}^{\rm I}$

In this section we present the details of the numerical calculations which we have performed to determine $Z_{\rm A}$ and $Z_{\rm V}$. We start in subsect. 5.1 by listing the expressions for f_1, $f_{\rm V}$ and $f_{\rm AA}^{\rm I}$ in terms of quark propagators. In subsect. 5.2 we briefly discuss the lattice action and algorithms used in the numerical simulation. We have closely followed the procedures outlined in ref. [18], which can be consulted for further information and any unexplained notations.

5.1 Explicit form of f_1, $f_{\rm V}$ and $f_{\rm AA}^{\rm I}$

As already mentioned in subsect. 3.4, the mathematical expressions corresponding to the quark diagrams shown in figs. 1 and 2 are obtained by applying Wick's theorem to the appropriate product of quark fields. There is only one diagram contributing to the correlation function f_1 and one finds that

$$f_1 = \tfrac{1}{2} \left\langle \, \mathrm{tr} \, \{ K^\dagger K \} \right\rangle_{\rm G} , \tag{5.1}$$

where the trace is over the Dirac and colour indices. The matrix K represents the quark propagation from the boundary at time 0 to the boundary at time T. In terms of the solution $H(x)$ of the lattice Dirac equation introduced in sect. 2

of ref. [18] it is given by

$$K = \frac{a^3}{L^3} \sum_{\mathbf{x}} \left\{ P_+ U(x,0)^{-1} H(x) \right\}_{x_0 = T-a} . \tag{5.2}$$

The numerical calculation of $H(x)$ is discussed in subsect. 3.2 of ref. [18].

In the case of the correlation function $f_{\rm V}(x_0)$, two diagrams contribute and one obtains

$$f_{\rm V}(x_0) = \frac{a^3}{2L^3} \sum_{\mathbf{x}} \left\langle \mathrm{Re\ tr} \left\{ K^\dagger \gamma_5 H'(x)^\dagger \gamma_5 \gamma_0 H(x) \right\} \right\rangle_{\rm G} , \tag{5.3}$$

where $H'(x)$ denotes the quark propagator from the boundary at time T to the point x in the interior of the space-time volume. $H'(x)$ is defined through the Dirac equation

$$(D + \delta D + m_0) H'(x) = 0, \qquad 0 < x_0 < T, \tag{5.4}$$

and the boundary conditions

$$P_+ H'(x)|_{x_0=0} = 0, \qquad P_- H'(x)|_{x_0=T} = P_- . \tag{5.5}$$

The numerical solution of these equations proceeds as in the analogous case of the matrix $H(x)$ (cf. subsect. 3.2 of ref. [18]).

Taking the definition (3.2) of the improved axial current into account, the correlation function $f^{\rm I}_{\rm AA}(x_0, y_0)$ may be expanded according to

$$f^{\rm I}_{\rm AA} = f_{\rm AA} + c_{\rm A} a \left[\tilde{\partial}_0^x f_{\rm PA} + \tilde{\partial}_0^y f_{\rm AP} \right] + c_{\rm A}^2 a^2 \tilde{\partial}_0^x \tilde{\partial}_0^y f_{\rm PP} \tag{5.6}$$

with the obvious definitions of $f_{\rm AA}$, $f_{\rm AP}$, $f_{\rm PA}$ and $f_{\rm PP}$. The superscripts on the symmetric difference operator

$$\tilde{\partial}_\mu = \tfrac{1}{2} (\partial^*_\mu + \partial_\mu) \tag{5.7}$$

imply a differentiation with respect to x or y respectively. As discussed in subsect. 3.4 only the diagrams a-d in fig. 2 need to be evaluated for the computation of $Z_{\rm A}$. The corresponding expressions for $f_{\rm AA}$, $f_{\rm AP}$, $f_{\rm PA}$ and $f_{\rm PP}$

look very similar and we only give the result for $f_{\rm AA}$ and diagram a, viz.

$$\{f_{\rm AA}(x_0,y_0)\}_{\rm diagram\ a} =$$

$$\frac{a^6}{4L^3}\sum_{\mathbf{x},\mathbf{y}}\left\langle\,{\rm tr}\,\left\{K^\dagger\gamma_5 H'(x)^\dagger\gamma_5\gamma_0\gamma_5 S(x,y)\gamma_0\gamma_5 H(y)\right\}\right\rangle_{\rm G}. \qquad (5.8)$$

The bulk quark propagator $S(x,y)$ appearing in this formula is the inverse of the Dirac operator $D+\delta D+m_0$ in the space of quark fields with vanishing boundary values. When evaluating $f_{\rm AA}$ and the other correlation functions, the propagator itself is however not required. Instead one first calculates $H(x)$ at all x and then solves the Dirac equation

$$(D+\delta D+m_0)\left\{a^3\sum_{\mathbf{y}}S(x,y)\gamma_0\gamma_5 H(y)\right\} = a^{-1}\delta_{x_0 y_0}\gamma_0\gamma_5 H(x) \qquad (5.9)$$

by applying the usual iterative methods.

5.2 Details of the simulation

As for the coefficients multiplying the O(a) counterterms in the improved action and the improved axial current, we follow ref. [18] and set

$$c_{\rm sw} = \frac{1-0.656\,g_0^2-0.152\,g_0^4-0.054\,g_0^6}{1-0.922\,g_0^2}, \qquad (5.10)$$

$$c_{\rm A} = -0.00756\,g_0^2\times\frac{1-0.748\,g_0^2}{1-0.977\,g_0^2}, \qquad (5.11)$$

for all couplings in the range $0\le g_0\le 1$. These formulae have been obtained non-perturbatively by imposing some carefully chosen improvement conditions. We expect that an almost perfect cancellation of O(a) effects in on-shell quantities is thus achieved.

From now on we shall often quote values of $\beta=6/g_0^2$ and $\kappa=(8+2am_0)^{-1}$ instead of the bare coupling and mass. All our production runs have been performed on APE/Quadrics computers with 256 nodes. We used the same hybrid over-relaxation algorithm as described in subsect. 3.1 of ref. [18] to generate a representative ensemble of gauge field configurations. Subsequent evaluations of the correlation functions f_1, $f_{\rm V}$ and $f_{\rm AA}^{\rm I}$ were separated by 25 iterations of the algorithm. We have checked explicitly for the statistical independence

of our sample by dividing the full ensemble into bins, each containing a number of individual "measurements". The statistical errors were then monitored as the number of measurements per bin was increased. We did not observe any significant change of the errors for increasing bin size, which we take as evidence for the statistical independence of our sample.

To invert the Dirac operator we employed the stabilized biconjugate gradient algorithm (BiCGstab) with even-odd preconditioning [19,20]. By comparing our results with those from a set of Fortran-90 programs, we have verified not only the correct evaluation of correlation functions, but also that the rounding errors associated with the 32 bit arithmetic on the APE computer were completely negligible in our calculation. All statistical errors were estimated using the jackknife method.

6. Computation of $Z_{\rm V}$ and $Z_{\rm A}$

We now proceed to describe the non-perturbative determination of the normalization factors $Z_{\rm V}$ and $Z_{\rm A}$ in the range $0 \leq g_0 \leq 1$. Except for the tests mentioned in subsect. 6.4, the boundary values C and C' of the gauge field and the angles θ_k are set to zero throughout this section.

6.1 Complete specification of the normalization conditions

As discussed in sect. 4 we need to make a definite choice for the parameters on which the normalization conditions (3.13) and (3.18) depend. The quark mass is set to zero, as previously indicated, and the remaining parameters are then the times at which the currents are inserted and the lattice extensions T and L. We scale these parameters proportionally to L and eventually decided to take

$$Z_{\rm V} f_{\rm V}(T/2) = f_1, \qquad T = 2L, \tag{6.1}$$

$$Z_{\rm A}^2 f_{\rm AA}^{\rm I}(2T/3, T/3) = f_1, \qquad T = 9L/4, \tag{6.2}$$

as the definite form of the normalization conditions. We still need to say, however, what precisely it means to set the quark mass to zero and how L/a is to be scaled with g_0.

The critical hopping parameter $\kappa_{\rm c}$ (i.e. the zero mass point) depends on the details of the lattice definition of the quark mass [16,18]. The ambiguity is just one of the sources of the order a^2 corrections in the normalization conditions for the currents and so is to be treated following the lines of sect. 4, i.e. we adopt any particular definition of the quark mass and use it to calculate $\kappa_{\rm c}$.

The definition that we have chosen is the same as the one previously employed in sect. 7 of ref. [18]. The starting point is the unrenormalized current quark mass $m(x_0)$ which one extracts from the PCAC relation (eq. (5.2) of ref. [18]). We then set $T = 2L$ and define $\kappa_{\rm c}$ to be the value of the hopping parameter κ where

$$m_{\rm av} = \tfrac{1}{5} \sum_{t=-2a}^{2a} m(T/2+t) \tag{6.3}$$

vanishes. The average over the time coordinate x_0 is taken to reduce the statistical error on the calculated mass values [18]. Note that the critical hopping parameter so defined is slightly dependent on L/a. It is implicitly understood that at any given value of β one chooses a lattice size L/a and first computes $\kappa_{\rm c}$ and then evaluates the normalization conditions (6.1) and (6.2) at this value of $\kappa_{\rm c}$ and the same lattice size L/a.

At this point the normalization constants $Z_{\rm V}$ and $Z_{\rm A}$ are well-defined functions of g_0 and L/a. The dependence on the lattice size is of order $(a/L)^2$ in the continuum limit and we have verified that at the couplings of interest the change in the calculated values of the normalization constants is indeed small when increasing L/a from say 8 to 16.

According to the discussion in sect. 4 we now need to make a definite choice of L/a. To ensure that the on-shell matrix elements of the renormalized improved currents approach the continuum limit with a rate proportional to a^2, we must require that L remains fixed in physical units. Explicitly, we define L/a at all couplings $g_0 \leq 1$ through

$$L/a = 8 \quad \text{at} \quad g_0 = 1, \tag{6.4}$$

$$L/r_0 = \text{constant}, \tag{6.5}$$

where r_0 denotes a hadronic scale extracted from the force between heavy quarks [21]. Using recent lattice data for r_0 [22] one finds that $L/a|_{\beta=6.2} \simeq 11$, $L/a|_{\beta=6.4} \simeq 14$ and $L/a > 16$ for $\beta \geq 6.8$. For practical reasons we did not perform the simulations at exactly these lattice sizes. In fact this is not really

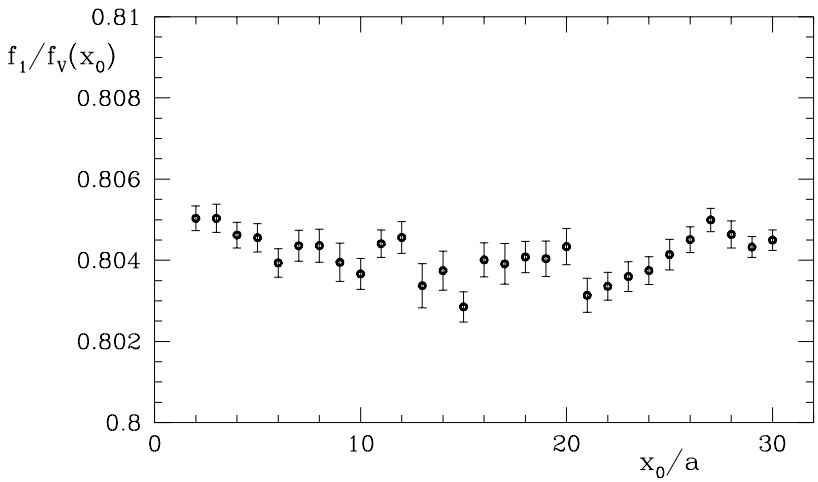

Fig. 3. Simulation results for $f_1/f_{\rm V}(x_0)$ from a lattice of size 32×16^3 at $\beta = 6.4$ and zero quark mass. Note that we are using a fine scale in this plot. The statistical fluctuations of the data points are on the level of a small fraction of a percent.

required because the associated systematic errors can be estimated reliably and turn out to be small (details are given below).

6.2 Results for $Z_{\rm V}$ and $Z_{\rm A}$

The statistical fluctuations of the numerators and denominators in the ratios $f_1/f_{\rm V}(x_0)$ and $f_1/f^{\rm I}_{\rm AA}(x_0,y_0)$ are strongly correlated. The jackknife error estimation accounts for these correlations and the ratios are obtained with impressive statistical accuracy even if only a small ensemble of independent gauge field configurations is available. Fig. 3 shows the ratio $f_1/f_{\rm V}(x_0)$ as a function of x_0/a from a typical run. One observes a clear signal with small statistical uncertainty and nearly no time-dependence within errors. The data points at different times x_0 are statistically decorrelated to such an extent that the signal-to-noise ratio can be enhanced by averaging the data in the range $T/2 - 2a \leq x_0 \leq T/2 + 2a$. Strictly speaking this should be taken as part of the definition of the normalization condition for $Z_{\rm V}$ (in the sense of sect. 4), but we did not want to obscure the discussion in subsect. 6.1 with too many details and thus mention this item only now. In the case of the ratio $f_1/f^{\rm I}_{\rm AA}(x_0,y_0)$ no averaging has been performed.

Table 1. The values of L/a and κ_c used in the normalization conditions

β	L/a	κ_c	L/a	κ_c
6.0	8	0.135046(16)		
6.2	8	0.135692(6)	12	0.135705(12)
6.4	8	0.135655(4)	16	0.135720(9)
6.8	8	0.135078(8)	16	0.135097(5)
7.4	8	0.134058(4)	16	0.134071(4)
8.0	8	0.133168(4)	16	0.133173(3)
9.6	8	0.131447(3)	16	0.131448(2)
12.0	8	0.129913(2)	16	0.129909(2)
24.0	8	0.127261(1)	16	0.127258(1)

In table 1 we list the values of β, the lattice sizes L/a and the associated critical hopping parameters κ_c at which the numerical simulations have been performed. Our final results for the normalization constants are collected in table 2. For each value of β we quote the number obtained on the larger lattice with two errors, the first being the statistical error, which includes the uncertainty in the value of κ_c quoted in table 1.

The second error is an estimate of the systematic effect which derives from the fact that the chosen lattice sizes are not exactly the ones required by the normalization conditions. The situation at $\beta = 6.0$ is exceptional in this respect, because $L/a = 8$ is the correct lattice size and the systematic error hence vanishes. The chosen lattice sizes $L/a = 12$ and $L/a = 16$ at $\beta = 6.2$ and $\beta = 6.4$ are rather close to the correct ones. In this case the data at $L/a = 8$ may be used to estimate the change in the normalization constants if L/a would be lowered to 11 and 14, repectively, which is then quoted as the systematic error in table 2. For $\beta > 6.8$ the error is taken to be the difference of the normalization constants calculated at $L/a = 16$ and $L/a = 8$. Since the effect is of order $(a/L)^2$ this procedure appears to be safe and presumably over-estimates the error.

Table 2. Results for $Z_{\rm V}$ and $Z_{\rm A}$

β	$Z_{\rm V}$	$Z_{\rm A}$
6.0	0.7809(6)	0.7906(94)
6.2	0.7922(4)(9)	0.8067(76)(23)
6.4	0.8032(6)(12)	0.8273(78)(10)
6.8	0.8253(5)(43)	0.8549(37)(73)
7.4	0.8494(3)(34)	0.8646(20)(48)
8.0	0.8667(2)(33)	0.8812(19)(17)
9.6	0.8973(2)(33)	0.9078(12)(37)
12.0	0.9232(2)(26)	0.9315(11)(16)
24.0	0.9656(1)(16)	0.9692(4)(14)

Our numerical results are also shown in fig. 4, where we compare them with the one-loop expressions [6,23,24],

$$Z_{\rm V} = 1 + Z_{\rm V}^{(1)} g_0^2 + {\rm O}(g_0^4), \qquad Z_{\rm V}^{(1)} = -0.129430, \tag{6.6}$$

$$Z_{\rm A} = 1 + Z_{\rm A}^{(1)} g_0^2 + {\rm O}(g_0^4), \qquad Z_{\rm A}^{(1)} = -0.116458. \tag{6.7}$$

These formulae describe the data rather well for, say, $g_0^2 \leq 0.5$, but in the range of couplings which is relevant for numerical simulations of physically large lattices this is no longer true.

The "mean field improved" perturbation expansion [25],

$$Z = u_0 \left\{ 1 + \left(Z^{(1)} + \tfrac{1}{12} \right) g_{\rm P}^2 + {\rm O}(g_{\rm P}^4) \right\}, \qquad Z = Z_{\rm V}, Z_{\rm A}, \tag{6.8}$$

comes much closer to the data at low values of β (see fig. 4). The expansion parameter here is Parisi's boosted bare coupling [26],

$$g_{\rm P}^2 = g_0^2 / u_0^4, \tag{6.9}$$

with u_0^4 being the average plaquette in infinite volume at the value of g_0^2 considered. We mention in passing that the data are nearly perfectly matched by the one-loop formulae (6.6) and (6.7) if we replace g_0^2 by $g_{\rm P}^2$.

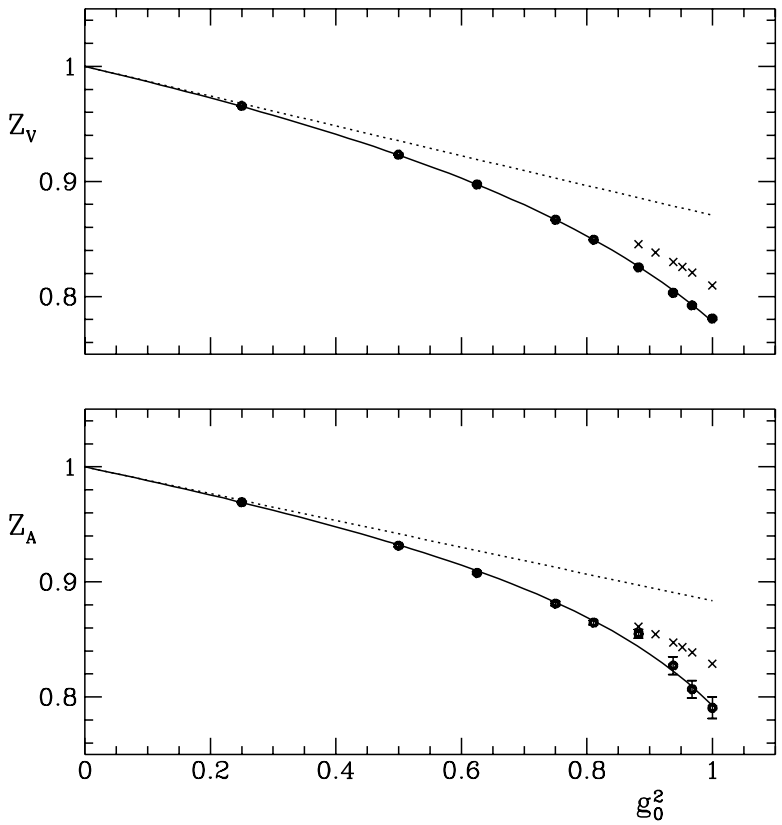

Fig. 4. Results for $Z_{\rm V}$ and $Z_{\rm A}$ from numerical simulations (filled circles), bare perturbation theory (dotted lines) and "mean field improved" perturbation theory (crosses). The solid lines represent the fits (6.10) and (6.11). For the numerical data only the statistical errors are displayed.

In the whole range $0 \leq g_0 \leq 1$ a good representation of the numerical results is given by the rational expressions

$$Z_{\rm V} = \frac{1 - 0.7663\, g_0^2 + 0.0488\, g_0^4}{1 - 0.6369\, g_0^2}, \tag{6.10}$$

$$Z_{\rm A} = \frac{1 - 0.8496\, g_0^2 + 0.0610\, g_0^4}{1 - 0.7332\, g_0^2}, \tag{6.11}$$

which coincide with the expansions (6.6) and (6.7) to order g_0^2. The fits repro-

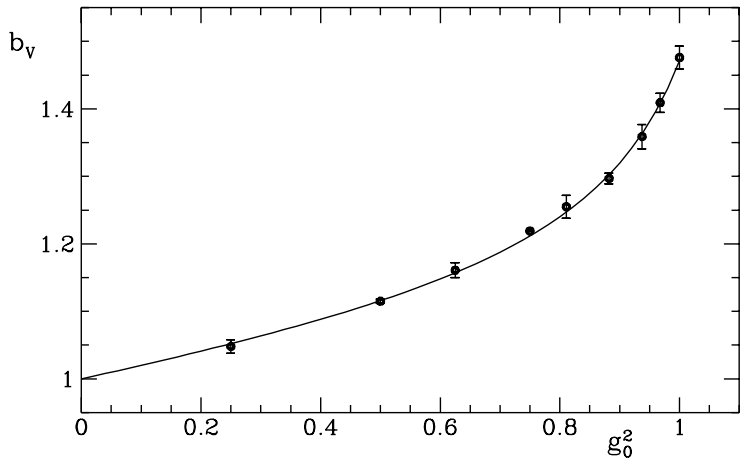

Fig. 5. Numerical results for the coefficient b_V. The solid line represents the fit (6.12).

duce the values of Z_V and Z_A quoted in table 2 with a precision better than 0.4% and 0.6%, respectively, an exception being the result for Z_A at $\beta = 6.8$ which deviates by 1.35%. Note, however, that the data points shown in fig. 4 are statistically independent and a statistical fluctuation of this size is hence not an unlikely event.

For future use of our results we suggest to either take the numbers quoted in table 2 (where this is possible) or else to employ the fit formulae given above, quoting an error of 0.5% for Z_V and 1.0% for Z_A. These error margins should be wide enough to account for all the uncertainties in our calculations.

6.3 Computation of b_V

At non-zero quark mass the renormalized improved currents involve correction factors of the form $1 + b_X a m_q$ that so far are only known to lowest order of perturbation theory [12,17]. The normalization condition (3.13) for the vector current, which is also valid for massive quarks, allows us to extract the coefficient b_V by studying the dependence of the ratio $f_1/f_V(x_0)$ on the quark mass m_q. In this subsection we report on our results for b_V obtained on lattices of size $L/a = 8$. At all couplings β considered we computed the correlation functions at several values of κ around κ_c and extracted b_V from the linear slope of $f_1/f_V(T/2)$ as a function of κ^{-1}. In the range $0 \leq a m_q \leq 0.005$ no significant curvature was observed in the data.

The results of our calculations are plotted in fig. 5. As in the case of the coefficients $c_{\rm sw}$ and $c_{\rm A}$, the data can be represented by a global fit

$$b_{\rm V} = \frac{1 - 0.6518\, g_0^2 - 0.1226\, g_0^4}{1 - 0.8467\, g_0^2}, \qquad 0 \le g_0 \le 1, \tag{6.12}$$

which reproduces the tree-level value $b_{\rm V} = 1$ at $g_0 = 0$.

For studies of pseudoscalar decay constants it would also be desirable to know the coefficient $b_{\rm A}$. The normalization condition for the axial current derived in subsect. 3.3 is however only applicable at zero quark mass. It is possible to deduce a more general normalization condition by taking the mass term in the PCAC relation into account, but the equation that one obtains involves a short distance contribution of order $am_{\rm q}$ which we would not know how to separate from the term proportional to $b_{\rm A}$. A more sophisticated approach is hence required to compute $b_{\rm A}$ non-perturbatively. We should add, however, that a perturbative estimate of $b_{\rm A}$ may be perfectly satisfactory, if one is interested in situations where $am_{\rm q}$ is small (say less than 0.01).

6.4 Residual cutoff effects in eqs. (3.13) and (3.18)

Now that the normalization constants $Z_{\rm V}$ and $Z_{\rm A}$ are known, we can ask how large the error term on the right-hand sides of eqs. (3.13) and (3.18) is for different choices of the kinematical parameters. In particular, we can vary the boundary values of the gauge field, the angles θ_k and the insertion points x_0, y_0, and we may also replace one of the quarks created and annihilated at the boundaries of the lattice by a strange quark with non-zero mass (cf. subsect. 3.4). The purpose of such studies is to verify the effectiveness of O(a) improvement and also to check that the particular choices made in subsect. 6.1 do not lead to uniformly large higher-order cutoff effects in other matrix elements of the renormalized currents.

Several tests, covering all variations mentioned above, have been performed at $\beta = 6.4$. For lattice sizes $L/a \ge 8$ we found that the cutoff effects would amount to changes in the normalization constants no larger than the statistical errors quoted in table 2, thus providing another impressive demonstration of the importance and effectiveness of improvement.

7. Concluding remarks

The computation of the current normalization constants $Z_{\rm A}$ and $Z_{\rm V}$ complements the non-perturbative determination of the O(a) counterterms in the improved action and the improved axial current reported in ref. [18]. In particular, physical matrix elements of the axial current in quenched QCD can now be obtained with O(a) improvement fully taken into account and small uncertainty in the normalization factor. It should again be emphasized, however, that an extrapolation to the continuum limit will always be required, even though we have not observed any significant residual cutoff effects in the matrix elements considered here.

The methods we have used in this paper carry over literally to QCD with dynamical quarks. As a first step one may be interested in a determination of the normalization constants using lattices of size $L/a = 8$ at all couplings g_0. The results obtained here suggest that the associated systematic errors are quite small (at most 2% in the case of $Z_{\rm A}$). Simulations of larger lattices will however be required for a reliable estimation of the systematic errors and for more precise results.

This work is part of the ALPHA collaboration research programme. We thank DESY for allocating computer time on the APE/Quadrics computers at DESY-IfH and the staff of the computer centre at Zeuthen for their support. We are also grateful to Peter Weisz and Ulli Wolff for helpful discussions and a critical reading of the paper. Stefan Sint is partially supported by the U.S. Department of Energy (contracts DE-FC05-85ER250000 and DE-FG05-92ER40742). Hartmut Wittig acknowledges the support of the Particle Physics and Astronomy Research Council through the award of an Advanced Fellowship.

Appendix A

We here deduce the Ward identity (3.14) assuming that the axial current is conserved (at zero quark mass) and that the operator product expansion is valid in a weak sense.

The axial current conservation amounts to saying that

$$\langle \partial_\mu A^a_\mu(x)\mathcal{O}\rangle = 0 \tag{A.1}$$

for any field product $\mathcal{O}$ localized in a region not containing x. It follows from this that the integral on the left-hand side of eq. (3.14) is independent of the region R (which must contain y and may not have any overlap with the localization region of $\mathcal{O}_{\rm ext}$). We may, for example, take R to be a ball with small radius r centred at y. For $r \to 0$ the integral may then be calculated by inserting the operator product expansion of $\epsilon^{abc}A^a_\mu(x)A^b_\nu(y)$. Up to logarithmic factors the contributions of the composite fields of dimension d are proportional to r^{d-3}. In particular, fields with dimension $d > 3$ make no contribution in the limit $r \to 0$. The only local field with dimension $d \leq 3$ and the appropriate transformation behaviour under the flavour and space-time symmetries is the vector current $V^c_\nu(y)$. We thus conclude that eq. (3.14) must be valid up to a proportionality constant k.

To prove that $k = 1$ we choose R to be the space-time volume between two equal-time hyper-planes and integrate over the space components of y. For $\nu = 0$ the left-hand side of eq. (3.14) is then equal to some matrix element of the commutator of the axial charge with itself, while on the other side of the equation one has a matrix element of the isospin charge between the same states. With the canonical normalization of the charges the matrix elements are the same and k must hence be equal to 1.

References

[1] M. Bochicchio et al., Nucl. Phys. B262 (1985) 331

[2] L. Maiani and G. Martinelli, Phys. Lett. B178 (1986) 265

[3] B. Meyer and C. Smith, Phys. Lett. 123B (1983) 62

[4] G. Martinelli and Zhang Yi-Cheng, Phys. Lett. 123B (1983) 433; ibid. 125B (1983) 77

[5] R. Groot, J. Hoek and J. Smit, Nucl. Phys. B237 (1984) 111

[6] E. Gabrielli et al., Nucl. Phys. B362 (1991) 475

[7] A. Borelli, C. Pittori, R. Frezzotti and E. Gabrielli, Nucl. Phys. B409 (1993) 382

[8] G. Martinelli, S. Petrarca, C. T. Sachrajda and A. Vladikas, Phys. Lett. B311 (1993) 241, E: B317 (1993) 660

[9] M. L. Paciello, S. Petrarca, B. Taglienti and A. Vladikas, Phys. Lett. B341 (1994) 187

[10] D. S. Henty, R. D. Kenway, B. J. Pendleton and J.I. Skullerud, Phys. Rev. D51 (1995) 5323

[11] G. Martinelli et al., Nucl. Phys. (Proc. Suppl.) 42 (1995) 428; Nucl. Phys. B445 (1995) 81

[12] G. Heatlie et al., Nucl. Phys. B352 (1991) 266

[13] G. Martinelli, C. T. Sachrajda and A. Vladikas, Nucl. Phys. B358 (1991) 212

[14] G. Martinelli, C. T. Sachrajda, G. Salina and A. Vladikas, Nucl. Phys. B378 (1992) 591

[15] K. Jansen et al., Phys. Lett. B372 (1996) 275

[16] M. Lüscher, S. Sint, R. Sommer and P. Weisz, Nucl. Phys. B478 (1996) 365

[17] M. Lüscher and P. Weisz, Nucl. Phys. B479 (1996) 429

[18] M. Lüscher, S. Sint, R. Sommer, P. Weisz and U. Wolff, Non-perturbative O(a) improvement of lattice QCD, CERN preprint CERN-TH/96-218 (1996), hep-lat/9609035

[19] H. van der Vorst, SIAM J. Sc. Comp. 12 (1992) 631

[20] A. Frommer et al., Int. J. Mod. Phys. C5 (1994) 1073

[21] R. Sommer, Nucl. Phys. B411 (1994) 839

[22] H. Wittig (UKQCD collab.), Nucl. Phys. B (Proc. Suppl.) 42 (1995) 288; private notes (1996)

[23] M. Göckeler et al., Perturbative renormalization of bilinear quark and gluon operators, Talk given at the 14th International Symposium on Lattice Field Theory, St. Louis, 4-8 June 1996, Humboldt Univ. preprint HUB-EP-96/39, hep-lat/9608033
[24] S. Sint, private notes (1996)
[25] G. P. Lepage and P. Mackenzie, Phys. Rev. D48 (1993) 2250
[26] G. Parisi, in: High-Energy Physics — 1980, XX. Int. Conf., Madison (1980), ed. L. Durand and L. G. Pondrom (American Institute of Physics, New York, 1981)